Journal of Inorganic and Organometallic Polymers and Materials (2020) 30:1306–1319
https://doi.org/10.1007/s10904-019-01307-9

Effect of M Nitrates on the Optical, Dielectric Relaxation and Porosity of PVC/PMMA Membranes (M = Cd, Co, Cr or Mg)

Gh. Mohammed[1,2] · Adel M. El Sayed[1,3] · S. El-Gamal[1,2]

Received: 20 May 2019 / Accepted: 29 August 2019 / Published online: 3 September 2019

Abstract
This work aims to study the influence of loading the inorganic nitrate salts of Cd, Co, Cr and Mg on the physical properties of the organic PVC/PMMA blend. The pure and composite (PVC/PMMA/nitrate salt) membranes were prepared via the casting technique. The structure, morphology, thermal, optical properties and dielectric relaxation of the samples were studied. XRD results showed that introducing the nitrate salts increase the films' amorphicity. FTIR spectra confirmed the complexation between the nitrate salts and the blend via hydrogen bonding. SEM revealed that the addition of Cd or Mg salt turned the blend surface from a fingerprint-like morphology to wrinkle-like appearance or sponge-like structure, respectively. Differential scanning calorimetry (DSC) confirmed the miscibility between PVC and PMMA and illustrated that loading these salts decrease the melting point T_m of the blend. UV–vis-IR spectroscopy showed that adding the Cd or Mg salts maintain transmittance > 80% in the visible region. Moreover, the added salts create semiconducting behavior for these films. The dielectric properties were studied in the frequency (f) range (10 Hz–20 MHz) at RT. The change of the ac conductivity (σ_{ac}) with f was analyzed in view of ac universality law. An increase in σ_{ac} with complexing nitrate salts was reported. The electrical modulus (M', M'') formalism predicts a non-Debye type conductivity relaxation and that the doped films are ionic conductors. Based on the obtained results, the obtained membranes are candidates for Cr and Co batteries application as well as water treatments and filtration process.

Keywords PVC/PMMA · Polymer/nitrates complexation · Band gap · Porous structures · Dielectric relaxation · Filtration membranes

1 Introduction

Recently, fabrication of polymer membranes for water purification, batteries, and other technological applications attained increasing attention worldwide. The usual routes to obtain membranes with specific properties involve blending two or more polymers and/or forming composites via mixing some metal salts with the blend [1–6]. The chosen polymers for blend formation should be miscible, combatable, and dissolve in the same solvent. Additionally, the added salts or dopants should be able to enhance the electric and opto-electronic properties of the host material without damaging or destroying its structure [7, 8].

Poly(methyl methacrylate) (PMMA), $[CH_2=C[CH_3]CO_2CH_3]_n$, has gained unlimited interest due to its high transparency, UV stability, low water absorption, and low refractive index. PMMA is rigid, hard, has a high electrical performance, thermoplastic, exhibits good outdoor weather resistance and resistance to hydrolysis [9, 10]. Avelino et al. improved the thermo-oxidative stability, and UV-blocking properties of PMMA by complexing with lignin [11]. PMMA-g-(Polyethylene glycol) (PEG) membrane formed in water exhibited higher permeability, smoother surfaces, higher porosity, and ~ 100% fouling reversibility compared with those formed in ethanol [12]. Mahant et al. [6] found that 50% (Polyvinylidene fluoride) (PVdF)/50% PMMA membrane has a high porosity, electrolyte uptake and ionic conductivity that make it a promising separator for Li-ion batteries. An ionic conductivity of ~ 4.62×10^{-3} S/cm at RT

✉ S. El-Gamal
samy_elgamal@edu.asu.edu.eg

[1] Physics Department, Faculty of Science, Northern Border University, Arar 91431, Saudi Arabia

[2] Physics Department, Faculty of Education, Ain Shams University, Roxy, Cairo 11757, Egypt

[3] Physics Department, Faculty of Science, Fayoum University, Fayoum 63514, Egypt

was achieved for the alumina-doped PVdF/PMMA by KI [13].

On the other hand, organic polyvinylchloride (PVC) is a commercial polymer with excellent mechanical, insulation properties and thermal stability, besides its recoverability [14]. The large chlorine content of PVC executes it relatively immune to ignition and burning [15]. These properties introduce PVC in various fields including the building construction, food packaging and electronic equipment [15]. Moreover, the strong chemical resistance to the inorganic acids, halogens, and alkalis, make PVC is an outstanding polymer for the ultrafiltration membranes. However, due to its high hydrophobicity, PVC suffers from fouling during the filtration processes [16]. Addition of 3 wt% alumina to PVC was found to increase its water permeability, the flux recovery and reduce its fouling [17]. PVC complexed with zinc molybdophosphate showed higher thermal stability than pure PVC [18]. Arslan et al. [19] prepared PVC/$Cu_3(PO_4)_2$ and polystyrene/$Ni_3(PO_4)_2$ ion exchange porous membranes with high stability, by a sol–gel route. da Silva et al. [20] reported that adding Copper Sulfide Nanoparticles increases the radiation stability of PVC. Bhran et al. [21] reported that the mechanical behavior of PVC was improved by blending with Poly(vinyl pyrrolidone) (PVP). PVC/PVP membranes can be applied for seawater treatment. $Mg(OH)_2$/lignin/PVC exhibited thermal stability three times higher than that of PVC and hence, the composite is more fire-resistant [22]. Arsalan et al. [23] studied the effect of $Co_3(PO_4)_2$ or $Ni_3(PO_4)_2$ on the thermal, dielectric and electrochemical properties of PVC. Zhao et al. [24] reported a conductivity of 3.57×10^{-3} S/cm at RT for 30% P(VC-VAc)/70% (PVdF) film, prepared via a phase inversion method.

PVC and PMMA are miscible up to 60 wt% of PMMA [25]. Such miscibility is owing to the hydrogen bonds involving the alpha hydrogen and the carbonyl group of PMMA [26]. PVC/PMMA blend attracts many investigators [27] and is commonly used in data cables, liquid crystal displays, [6] and various electronic applications [27]. Blending PVC and PMMA improve the mechanical, structural and thermal properties of PVC [28, 29]. Other investigators add some metal salts [27, 30] or metal oxides [31] to enhance the blend properties and widen its applications. PVC and PMMA have polar groups so they have high dielectric constant and can form polymer–salt complexes.

Based on the last-mentioned survey, PVC/PMMA blend can be used in a different industrial field based in polymer membranes. The influences of nitrates of Cd, Co, Cr, and Mg on the morphological, optical and electric properties of PVC/PMMA are discussed, for the first time, as a comparative study. The structural properties of the membranes were investigated by XRD and FTIR spectroscopies as well as SEM microscopy. In addition, different optical and electric parameters were evaluated and discussed.

2 Experimental Procedures

2.1 Materials and Preparation

PVC (Polymer Laboratories, UK), and PMMA, 3.5×10^4 g/mol, Acros Organics, were used for the blend preparation. Tetrahydrofuran (THF, Aldrich, Germany) was used as the solvent. $Cd(NO_3)_2{\cdot}4H_2O$ (308.47 g/mol, LOBA Chemie), $Co(NO_3)_2{\cdot}6H_2O$ (291.03 g/mol, Sigma), $Cr(NO_3)_3{\cdot}9H_2O$ (400.15 g/mol, LOBA Chemie), and $Mg(NO_3)_2{\cdot}6H_2O$ (256.41 g/mol, Uniwin Chemical Co., Ltd), were the inorganic salts used as additives. These salts were put in a hot furnace at 50 °C for 8 h to reduce the water content before use. The pure blend was prepared by dissolving 0.8 g PVC and 0.2 g PMMA in 80 mL THF with continuous stirring for 2 h at RT till the complete dissolution of the blend. The other films were prepared by adding about 0.11 g of each salt to the blend solution. The aqueous mixtures were cast into glass Petri dishes put in the air for solvent evaporation at RT. Care was taken to obtain homogenous membranes.

2.2 Measurements

X-rays diffraction of the pure and loaded blend was obtained using a PANalytical's X'Pert PRO. The vibrational properties of the PVC/PMMA functional groups were studied by Fourier transform infrared (FTIR) spectroscopy, using (JASCO, FT/IR-6200) in the wavenumber range 4000–400 cm^{-1}. The surface morphology combined with the cross-sectional investigation and films' thickness were checked using scanning electron microscopy (SEM), JEOL. The thermal properties were done via using the DSC technique (DSC; Shimadzu DSC-60) in the temperature range RT—400 °C with a heating rate of 10 °C/min in a nitrogen atmosphere. About 5 mg of each film was placed in sealed Aluminum pans. Prior to use, the instrument was calibrated with Aluminum oxide standard. The accuracy of the heat flow was ± 0.01 mW. Optical transmittance and absorbance spectra of the samples were recorded using a Jasco V-670 spectrophotometer in the wavelength range 200–1600 nm with an accuracy of ± 0.2 nm. Dielectric properties (ε', ε'' and tan δ) were recorded by a Hikoi (Ueda, Nagano, Japan) model 3532 High Tester LCR, in the frequency range 10 Hz–20 MHz, with capacitance measurement accuracy on the order of 1×10^{-4} pF, at RT.

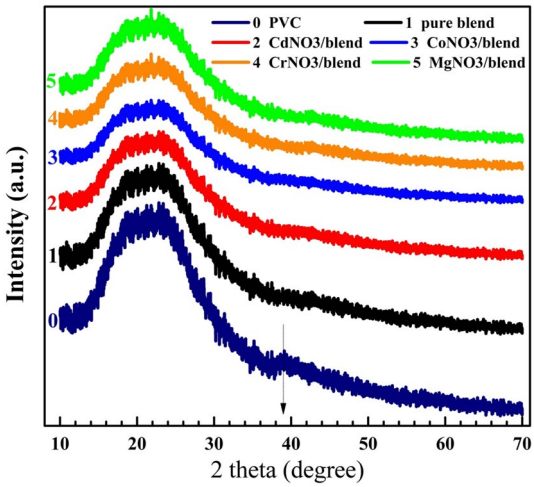

Fig. 1 XRD patterns of PVC, PVC/PMMA blend and the blend loaded with Cd, Co, Cr, and Mg nitrate

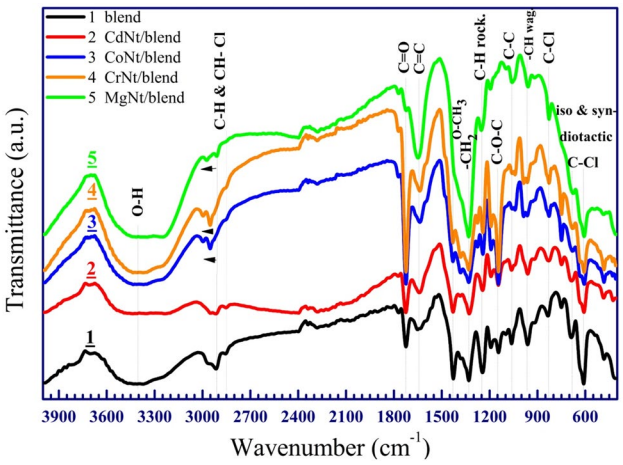

Fig. 2 FTIR transmittance spectra of PVC/PMMA blend and the blend doped with nitrate salts

3 Results and Discussions

3.1 XRD

XRD patterns of PVC, pure PVC/PMMA blend and the blend loaded with 10 wt% of the Cd, Co, Cr, and Mg salts are shown in Fig. 1. The amorphicity of pure PVC film is indicated by the existence of a broad peak in the 2θ region (12°–35°). However, the small peak at 39° indicates some ordering character in PVC. Similar results were reported in Ref. [32]. Blending PMMA with PVC disappeared this peak and made the main peak broader. This indicates that the blend is more amorphous compared to PVC. Similarly, although the β phase of PVdF has known peaks at 20.268° and 39.89°, PMMA/PVdF blend displayed only one peak at ~ 20.26° [10]. Moreover, the films' amorphicity has increased after loading with 10 wt% salt. The absence of any crystalline peaks for Cr, Co, Cd and Mg or salts indicates the complete complexation between these salts and the blend in its amorphous phase [30]. This rise in the films' disorder is expected to improve their optical and electric conductivities.

3.2 FTIR

To obtain information about the miscibility of PVC and PMMA as well as the complexation in the blend/salt membranes, FTIR spectroscopy was done as shown in Fig. 2. The spectrum of the pure blend exhibits a broad band centered at 3400 cm^{-1} and assigned to stretching of the O–H group. The existence of this band confirms the presence of moisture [33]. The intensity of this band decreased after $CdNO_3$ addition but enhanced in the other films. The two adjacent bands at ~ 2920 and ~ 2857 cm^{-1} for the blend are due to the asymmetric and symmetric vibration of $–CH_3$, $–CH_2$ and –CH–Cl groups [11, 31, 34]. After mixing the nitrate salts, these two peaks shifted to a relatively higher frequency, as indicated by small arrows. The two bands at 1725 and 1629 cm^{-1} are assigned to the asymmetric stretching of C=O group of organic PMMA and the symmetric C=C stretching of PVC, respectively [35, 36]. No shifts are observed after salts addition. The intensity of these two peaks increased simultaneously for the blend modified with Cd, Co, and Cr salts. However, Mg salt addition increased the intensity of C=C band at the expense of the intensity of C=O. The band at 1438 cm^{-1} is arising from $O–CH_3$ asymmetric bending mode of PMMA. While the band at 1325 cm^{-1} originating from the overlapping of CH_2 wagging in PMMA and CH_2 deformation mode of PVC cm^{-1} [6]. The last two peaks are weakened by Cd, Co, and Cr salts addition. Adding of $MgNO_3$ greatly improved the band 1325 cm^{-1} and at the same time eliminated the band at 1438 cm^{-1}. These results show that Mg salt interacts with the blend differently to that of the other salts.

The bands 1247 cm^{-1}, 1151 cm^{-1} and 1067 cm^{-1} are assigned to the C–H rocking, C–O–C absorption, and the stretching vibration of C–C bonds, respectively [34]. The band at 962 cm^{-1} is of CH_2 wagging vibration. The frequency at 829 cm^{-1} is assigned to symmetric C–Cl stretching [35]. The two adjacent bands at 687 and 610 cm^{-1} demonstrate the C–Cl bond of the isotactic and syndiotactic structure of PVC [34, 37]. The intensity of these two peaks for the investigated films is lower than that of the pure blend. This confirms the formation of H bonding between the salts and the blend.

3.3 SEM Analysis

Figure 3 shows the films' surface and edges morphology. The pure blend displays a dense, smooth, non-porous or cracked surface of fingerprint-like morphology. In addition, there are no apparent interfaces between PMMA and PVC indicating the good miscibility of the blend. 10 wt% $CdNO_3$ induced some roughness to the surface and a wrinkle-like appearance without visible cracks or pores. Doping with $CoNO_3$ created pores of non-uniform shape, sizes or distribution. A similar result for $CrNO_3$/blend film, but with relatively smaller pores and presence of linear/branched cracks on the film's surface. $MgNO_3$ addition improved the formation of pores throughout the film. The surface appears rough with a sponge-like structure. Similar results were reported for PVC/PMMA pure blend and blend loaded with nano-sized GeO_2 [34]. The average thickness of the pure membrane is 105.5 µm,

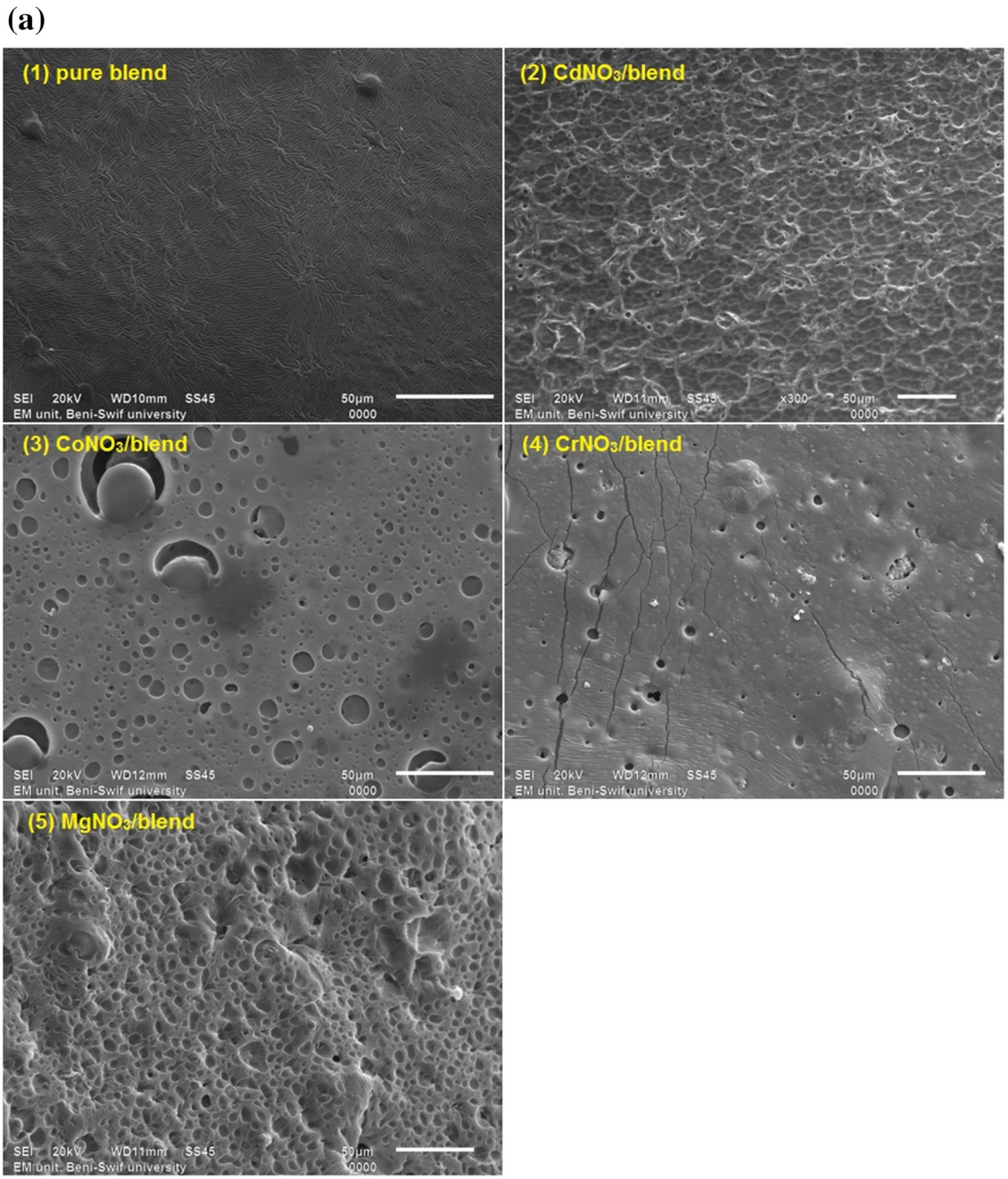

Fig. 3 **a** SEM analysis (top-surface) of PMMA/PVC/nitrates membranes. **b** SEM analysis (cross-section) of PMMA/PVC/nitrates membranes

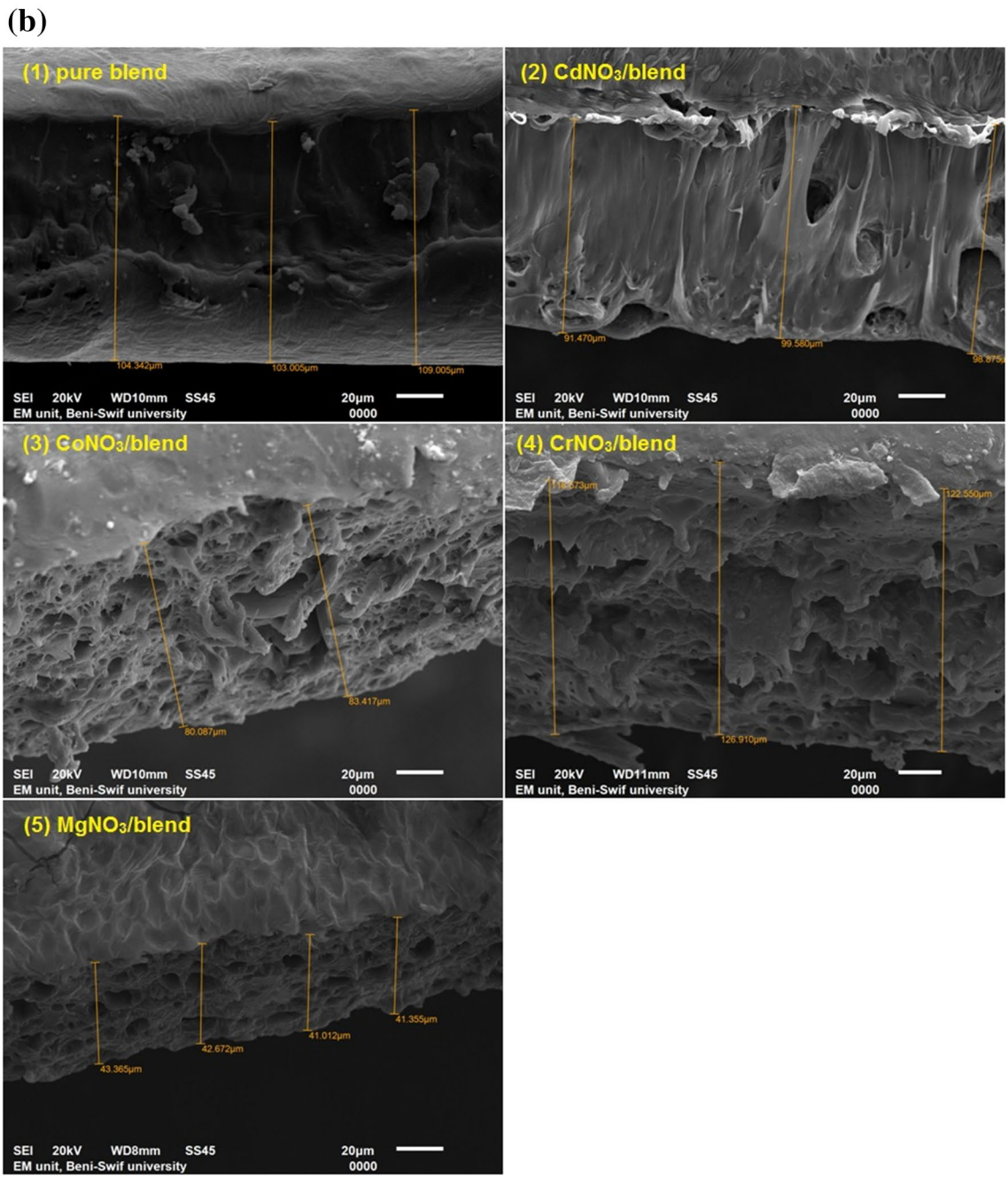

Fig. 3 (continued)

decreased to 96.6 µm, 81.8 µm, and 42.1 µm for the blend mixed with Cd, Co, or Mg nitrates, respectively. However, $CrNO_3$/blend membrane has 122.67 µm thickness. This indicates that all types of added salts interact differently in the PVC/PMMA/THF solution. As seen, the size of the pores throughout the edges is larger than that of the films' surfaces. These asymmetric structures, i.e. a dense top surface on a porous interlayer, make these membranes candidate for filtration applications [17].

Figure 4 shows the three porous membranes; Co, Cr, and Mg nitrates/blend at a higher magnification. Many circular pores of diameters in the range 1–14.65 µm are appearing on the surface of $CoNO_3$ doped blend. The pores on the $MgNO_3$/blend are more uniform in size. Cr salt introduced a small number of pores with the smallest average diameters. The observed micron-sized spherical pores are a result of the solvent evaporation and indication of the amorphicity of the membrane. These pores increase the electrolyte uptake,

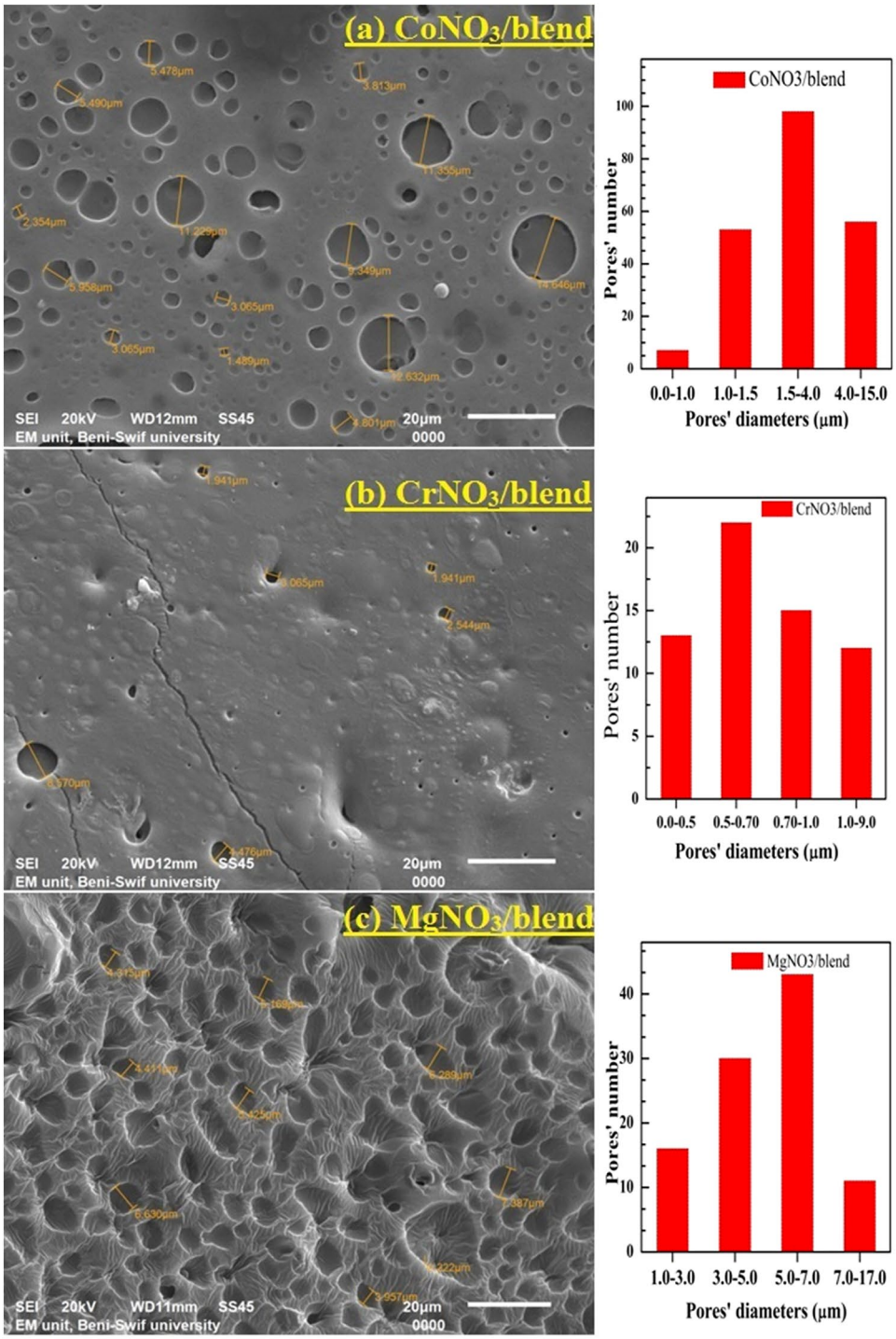

Fig. 4 **a**–**c** Top surface of the porous membranes at higher magnification (the left) and pores size/distribution (the right)

provide pathways for fast ions transport and enhance the membrane ionic conductivity. Therefore, these membranes could be used as separators in liquid batteries [38].

3.4 DSC Analysis

DSC is one of the most effective thermal techniques in investigating the thermal transitions & the miscibility in polymeric materials [39, 40]. DSC curves of PVC/PMMA blend and PVC/PMMA loaded with 10 wt% nitrate salts in the temperature range 30–400 °C are elucidated in Fig. 5. The broad exothermic peaks that appeared in some films in the temperature range, 130–180 °C, were assigned to the relaxation associated with the crystalline regions in the investigated films [41], see T_C values in Table 1. The endothermic peak at about 288.8 °C was assigned to the melting

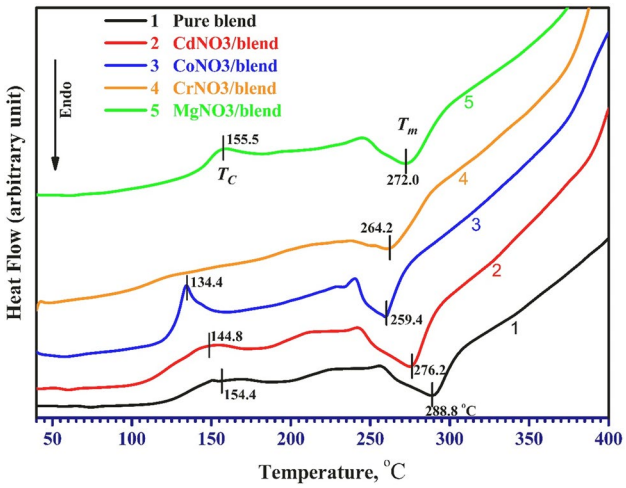

Fig. 5 DSC spectra of PVC/PMMA blend and the blend doped with nitrate salts

point of the PVC/PMMA blend. This value is higher than the reported one by Alghunaim [3], 278.9 °C, which refers to the difference in the blend composition. On the other hand, observing one T_m of the blend confirms the miscibility between its constituents [40], in other words, we have a homogeneous film structure. A decrease in T_m values was observed with complexing with different metal nitrate salts, see Table 1. T_m decrement confirms the interaction between metal salts with PVC/PMMA blend matrix, as confirmed by FTIR. It is owing to the reduction in the ordered association of the blend with salt complexation which causes a decrease in the blend crystallinity [39]. This suppose agrees with XRD observations. No decomposition of the studied films was reported up to 400 °C which may be due to an increase in their thermal stability.

3.5 Optical Characterization

Figure 6a depicts the transmittance (T %) of the PMMA/PVC membrane loaded with different nitrate salts. The T % value in the visible part of the spectra is around 80% for the pure blend, increased very slightly for Mg/blend and to 86% for Cd/blend. However, doping with Co and Cr salts decreased T % to be in the range 62–74% and 50–85%, respectively. These salts shift the absorption edge to higher wavelengths. Moreover, Cr/blend do not permit any light transmission before 300 nm wavelength. Figure 6b shows

Table 1 The melting temperature, T_C, indirect and direct optical bandgap and Urbach energy (E_U) for the pure PVC/PMMA membrane and PVC/PMMA loaded with 10 wt% nitrate salts

Film	T_m (°C)	T_C (°C)	Indir. E_g (eV)	Dir. E_g (eV)	E_U (eV)
PVC/PMMA (blend)	288.8	154.4	4.3	4.9	0.53
$CdNO_3$/blend	276.2	144.8	4	4.6	0.55
$CoNO_3$/blend	259.4	134.4	2.1	3.7	1.723
$CrNO_3$/blend	264.2	–	1.9	3.4	1.56
$MgNO_3$/blend	272	155.5	4.2	4.8	0.52

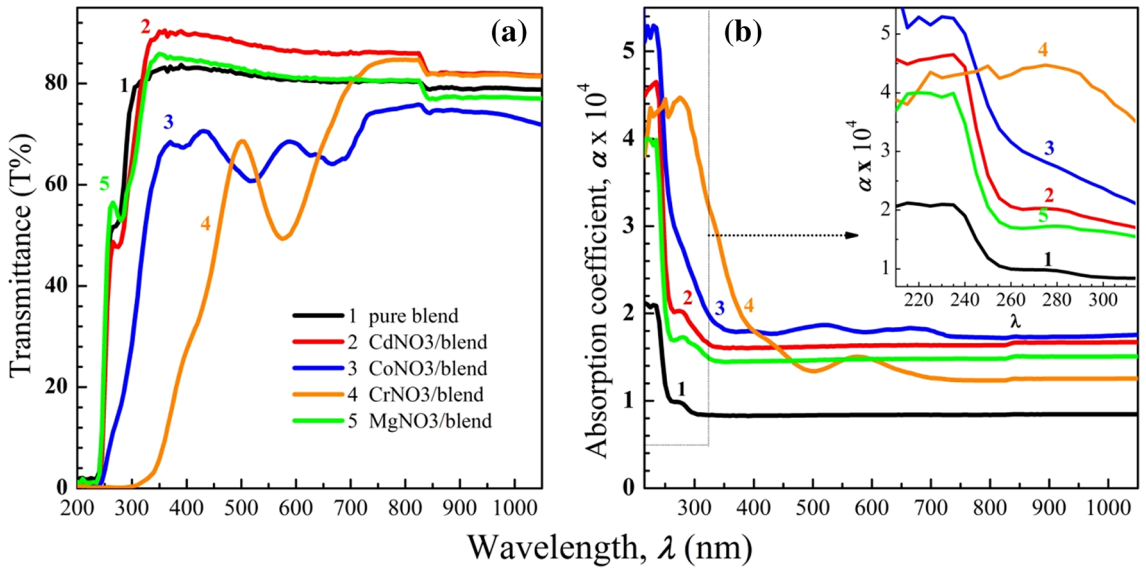

Fig. 6 The optical transmission spectra (**a**) and the absorption coefficient (**b**) of the pure and doped membranes

the absorption coefficient ($\alpha = Abs./film's\ thickness$). As seen, α for any blend/salt film is higher than that of the pure blend. This is owing to the pore network that can enriches the absorption property of the porous membranes through the polarization of electromagnetic waves [34]. The sharp increase in α at $\lambda < 260$ nm is owing to the C–Cl bond [32]. The absorption peaks between 225 and 235 nm is assigned to $\pi \rightarrow \pi^*$ transitions due to the presence of C=O unsaturated bonds [3]. Another absorption band for the pure blend and that loaded with Co, Cr and Cd nitrates is observed at 275 nm and shifted to 280 nm for Mg/blend film. This shift is attributed to the interaction between the blend chains and Co, Cr and Cd ions. Similar observations were reported for poly(pyrrole–co–N-methylpyrrole)–ZnO_2 [42].

Figure 7a, b shows the indirect and direct optical bandgap (E_g) of the membranes calculated using Tauc's relation; $(\alpha h\upsilon)^{\frac{1}{m}} = A\left(h\upsilon - E_g\right)$, where $h\upsilon$ is the photon energy, A is a constant, and $m = 2$ and 1/2 for the indirect and direct allowed transitions, respectively. The indirect and direct E_g of the pure blend are 4.3 and 4.9 eV, respectively. Adding Mg and Cd nitrate salts decreased these values, as listed in Table 1. Co and Cr nitrates, however, significantly narrowed E_g of the blend to be in the range 1.9–2.1 eV and 3.4–3.7 eV for the indirect and direct E_g, respectively. Alghunaim [3] reported the decrease of direct E_g of this blend from 5.01 to 3.92 eV after doping with 10 wt% $CoCl_2$. Sangawar and Moharil reported 60–70% transmission in the visible region and indirect E_g of 3.21 eV for (80% PVC/20% PMMA) [43]. Mohammed [10] reported a direct E_g for PVDF/PMMA of 5.85 eV, decreased to 5.65 eV after doping with 10% ZnO nanoparticles. Nadimicherla et al. [44] found that the indirect and direct E_g of PVC(50%)/PEO(50%) blend are 4.15 and 4.10 eV and reduced to 3.22 and 3.24 eV, respectively after mixing with 10% KI. As indicated in XRD and SEM results, the added nitrate salts increase the disorder character inside the membranes and the formed pores represent pathways for the movement of free charges.

The width of the exponential absorption edge or the Urbach energy (E_U) is related to α by the relation [45]; $\alpha = \alpha_o \exp\left(\frac{h\upsilon}{E_U}\right)$. This equation can be rewritten as $\mathrm{Ln}(\alpha) = \mathrm{Ln}\left(\alpha_0\right) + \frac{h\upsilon - r}{E_U}$, where α_0 and r are constants. E_U is the inverse of the slope of the curves shown in Fig. 8, and its values are listed in Table 1. Increasing E_U is an indication of increasing the disorder in our membranes. E_U of the pure blend is 0.53 eV. Loading the nitrate salts led to states' redistribution from the band to tail and allowing an increasing number of band-to-tail and tail-to-tail transitions. This result is consistent with XRD and SEM analysis.

3.6 Dielectric Properties

The dielectric measurements are frequently carried out to investigate the relaxation behavior and ac conduction mechanism in polymeric materials [46, 47]. As known, the dielectric constant ε' is a direct measure of the stored charge inside the blend while the dielectric loss ε'' expresses the dissipation of energy due to Joule's heating effect. This is done by migrating or rotating the molecules when subjected to an electric field. Hence, the dependence of both ε'' and tan δ $(= \varepsilon''/\varepsilon')$ of the films on the applied frequency f will be reported.

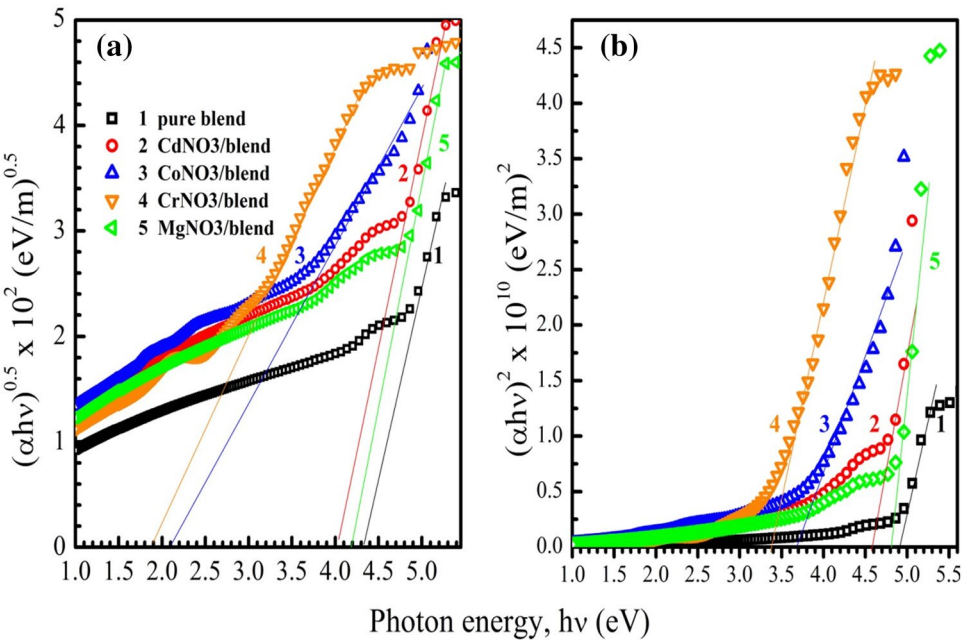

Fig. 7 The indirect (**a**) and the direct (**b**) bandgap calculation (Tauc's plots) of the pure and doped membranes

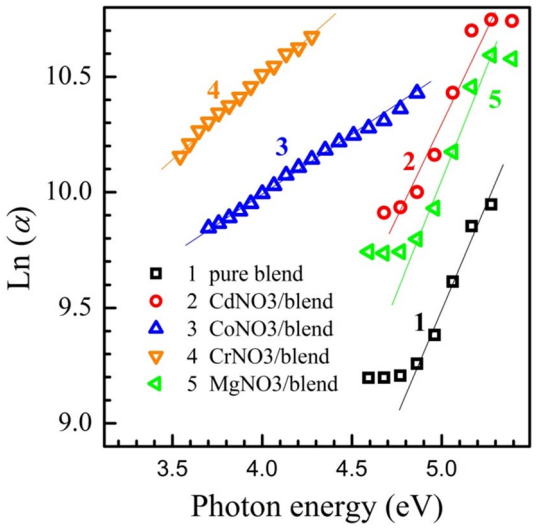

Fig. 8 Urbach energy (E_U) determination for the prepared membranes

3.6.1 Dielectric Constant and Dissipation Factor Study

The plots of ε' of the PVC/PMMA blend, the inset, and the synthesized blend/salt films at different frequencies f (10 Hz–20 MHz) and at RT are shown in Fig. 9a. The rise in ε' at the low f is referred to the ability of dipoles in the blend film to orient themselves in the direction of the applied field. With increasing f, these dipoles fail to follow the change in the applied field, so ε' decreases. The value of ε' of the blend at 10 Hz is about 3 and increased, for example, to 291 when complexed with $CrNO_3$. Such significant increase is owing to (i) the free charges that build-up at the electrode-film interface which encourages the dipoles to orient themselves in the electrolyte [14] (ii) the conversion of the medium to a heterogeneous one and consequently the interfacial polarization (IP) plays a great role [48].

The change of tan δ versus f of the pure blend and blend/salt films is depicted in Fig. 9b. The accumulation of free charges near the electrodes causes the higher values of tan δ at low f. While, the decrease in tan δ with f reflects the decrease in the polarization resulted from the decrease in charge build-up with increasing f. One peak is observed indicating the existence of relaxing dipoles. On the other hand, tan δ increases with salt complexation and this refers to the enhancement of the free charge motion within the blend matrix. In general, the shift in peak position to higher f indicates the reduction of the relaxation time and the peak broadening reflects the overlapping of interfacial polarization (IP) relaxation process and the merged α-, β-relaxation processes [49]. In the present work, more details about the relaxation processes will be discussed in the dielectric moduli section.

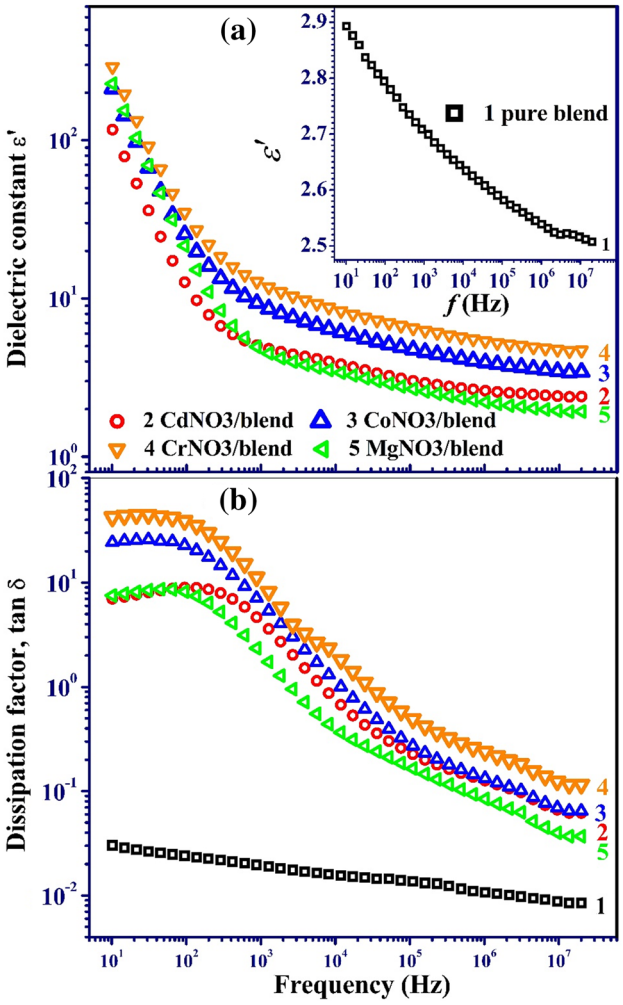

Fig. 9 Frequency dependence of **a** the dielectric constant ε'; **b** the dissipation factor tan δ for of PVC/PMMA and electrolyte films

3.6.2 AC Conductivity Measurements

The variation of AC conductivity (σ_{ac}) of the pure blend and blend/salt films with increasing f is shown in Fig. 10a while the dependence of σ_{ac} on the salt type at 52.4 kHZ, 1 and 4.5 MHz is plotted in Fig. 10b. Two regions were observed in Fig. 10a. Region I, the frequency independent plateau region, it is in correspondence with the dc conductivity [50]. Region I indicates the resistive conduction through the blend/salt films. This behavior is owing to IP, i.e., there is a charge accumulation at the electrode–film interfaces and consequently the number of charge carriers available for transportation is decreased leading to the semi-stability in σ_{ac}. However, a significant increase of σ_{ac} with increasing f was observed in Region II. At higher f, the mobility of charge carriers is enhanced and eventually contribute to higher ionic conductivity [51]. The change of σ_{ac} with f could be analyzed in view of ac universality law [52], $\sigma_{ac}(\omega) = \sigma_{dc} + A(\omega)^s$, where σ_{dc} is the frequency independent

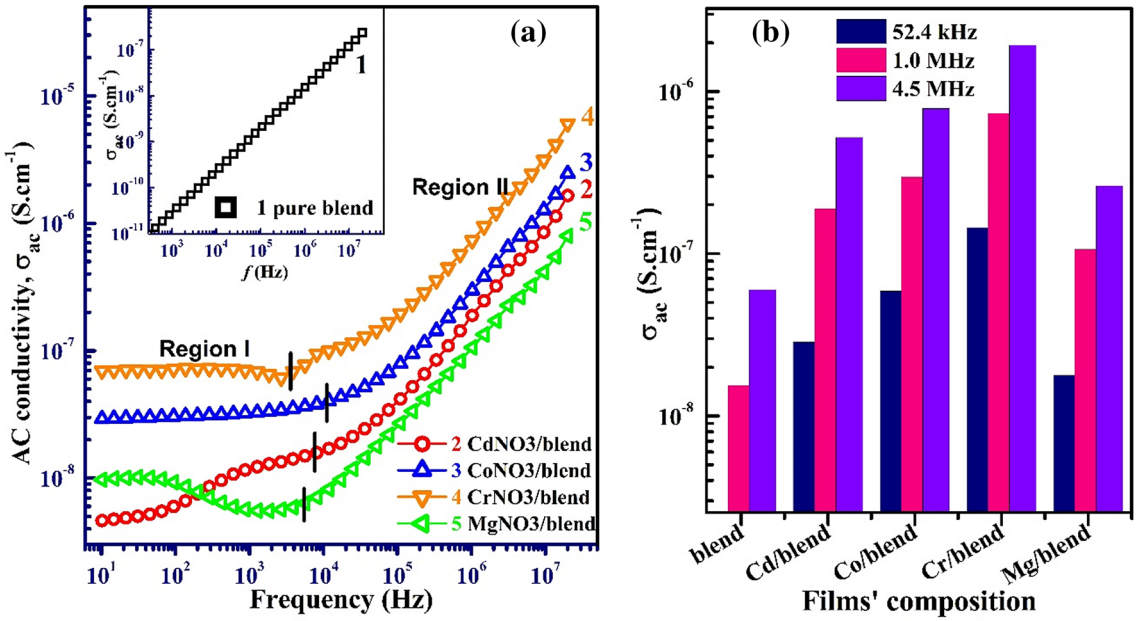

Fig. 10 **a** AC conductivity σ_{ac} as a function of frequency for the pure blend and electrolyte films, **b** values of σ_{ac} of the prepared films at some selected frequencies 52.4 kHz, 1 and 4.5 MHz

Table 2 dc conductivity (σ_{dc}), stretching parameter (β), power law exponent (s) and relaxation time (τ_M) of the pure blend and the blend/M nitrates films

Film	σ_{dc} (S/cm)	S	β	τ_M (sec.)
PVC/PMMA (blend)	4.01×10^{-14}	0.91	–	–
$CdNO_3$/blend	5.92×10^{-9}	0.6	0.542	5.94×10^{-5}
$CoNO_3$/blend	2.29×10^{-8}	0.67	0.569	9.26×10^{-6}
$CrNO_3$/blend	5.24×10^{-8}	0.65	0.404	4.41×10^{-6}
$MgNO_3$/blend	4.11×10^{-9}	0.37	0.538	1.95×10^{-5}

dc conductivity, i.e., σ_{ac} at zero Hz, ω is the angular frequency, A is a pre-exponential constant, and s is the power law exponent. The values of σ_{dc}, by extrapolating the plateau region to zero Hz, A, and s for the different films are presented in Table 2. As clear, the values of s lay in the range 0.37–0.91. $CrNO_3$ and $CoNO_3$ have higher values of s compared to other salts. In addition, there is a consistency between the calculated σ_{dc} and σ_{ac} with respect to the effect of salts complexation. In the present work, the maximum value of σ_{ac} was for Cr/blend which equals 6.05×10^{-6} S/cm at 20 MHz compared to 2.37×10^{-7} S/cm for the blend. This value is greater than the reported one by Sim et al. where they found that the complexation by $LiCF_3SO_3$ salt increases the ionic conductivity of PEMA/PVdF-HFP blend up to 4.13×10^{-7} S/cm [53]. But it is smaller than the value of 2.23×10^{-5} S/cm that was reported by Khan and Wahid [30] for PVC/PMMA loaded with 15 wt% of $LiClO_4$ salt at RT. Arunkumar et al. [35] reported a value of 1.16×10^{-4} S/cm for PVC/poly(butyl methacrylate) (PBMA)/$LiClO_4$ films increased to 7.12×10^{-4} S/cm after loading 10 wt% Al_2O_3 particles. Yanilmaz and Zhang [38] reported a value of 3.2×10^{-3} S/cm for PMMA/PAN (50/50) membrane films prepared by centrifugal spinning and checked their use as separators in Li-ion batteries.

As a summary, complexing the blend with metal salts increases σ_{ac} in general in the ascending order $MgNO_3$, $CdNO_3$, $CoNO_3$, and $CrNO_3$ salt doped films, see Fig. 10b. These salts increase the free charges within the pure blend. They increase the disorder/amorphous character and create pores, as confirmed by XRD and SEM. These encourage the charge motion within these pores' pathways. In addition, there is a good correlation between the values of optical band gaps, direct & indirect, and the σ_{dc} values as listed in Tables 1 and 2. For example, the blend/$CrNO_3$ film has the lowest indirect E_g value, 1.9 eV, and the highest σ_{dc}, 5.24×10^{-8} S/cm.

3.6.3 Dielectric Moduli Studies

The complex electric modulus formalism has been used for further analysis of dielectrics data by suppressing the polarization effects of the electrode. This gives more information about the relaxation processes. As known, the electric modulus M^* is defined as $M^*=\frac{1}{\varepsilon^*}=M'+j\,M''$ where ε^* is the dielectric permittivity, M' and M'' are real and imaginary parts of the electric modulus, respectively.

$$M' = \frac{\varepsilon'}{\left[(\varepsilon')^2 + (\varepsilon'')^2\right]}, \tag{1}$$

$$M'' = \frac{\varepsilon''}{\left[(\varepsilon')^2 + (\varepsilon'')^2\right]}. \quad (2)$$

Figure 11a, b shows M' and M'' moduli of the pure blend and blend/salt films as a function of the angular frequency ω ($=2\pi f$) at RT. As clear, the increase in M' with increasing ω indicates that the conduction in the blend/salt is assigned to ions. The zero value of M' and M'' at lower f side is due to the high capacitance accompanied by the electrode polarization [37]. Besides, it gives evidence on the non-Debye behavior in the investigated blend/salt, i.e., the conduction here depends on the viscoelastic and dipolar relaxations beside the free ions [54]. M'' exhibits a relaxation peak at the middle region of ω, see Fig. 11b. Before this peak, long-range mobility was suggested, however, after it, the ions were spatially confined in a narrow potential well, i.e., short-range mobility [55]. The presence of relaxation peaks in the modulus formalism confirms that the films are ionic conductors [56]. There is a peak shift towards higher ω when

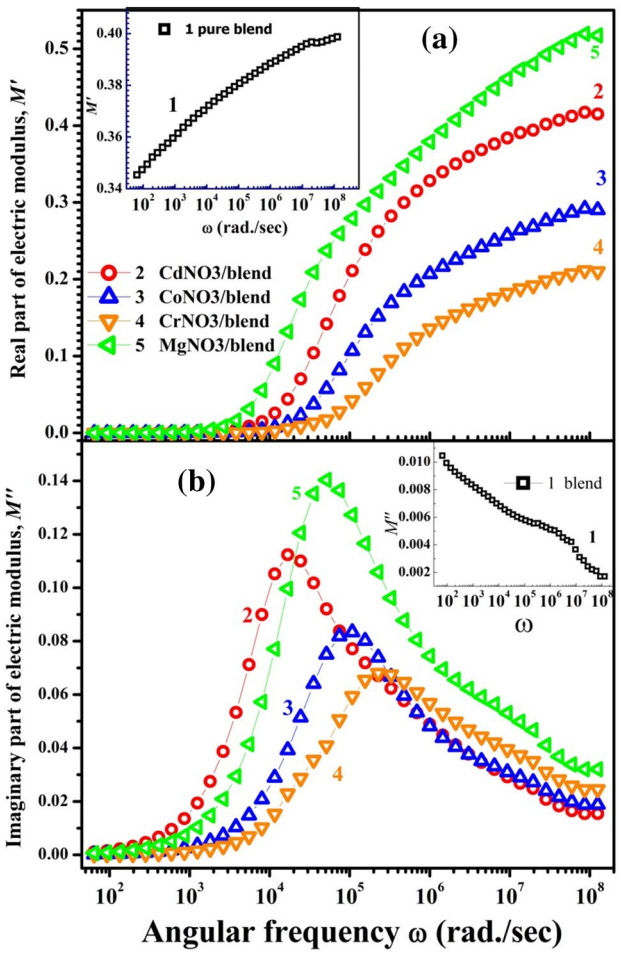

Fig. 11 Variations of M' and M'' versus frequency for the pure blend and electrolyte films

doping $CrNO_3$ and $CoNO_3$, compared to the other salts. This suggested an improvement in both the charge carriers' motion and the hopping probability of ions from one site to another one. A similar feature has been reported by Khutia and Joshi [31] when applied DC bias voltage (0–25 V) across PVC/PMMA/NiO films. It was noted that M'' of Cr and Co salts is lower than that of Mg and Cd salts. This may owe to the plurality of relaxation mechanism in $CrNO_3$/blend and $CdNO_3$/blend films [28]. The relation between M'' with ω, Fig. 11b, could be analyzed in view of the relaxation function φ_t suggested by Kohlrauch–Williams–Watts [57];

$$\varphi_t = \exp\left[-\left(\frac{t}{\tau_M}\right)^{\beta}\right], \quad (3)$$

where β is an exponent having values from 0 to 1 and indicates the departure from Debye relaxation [54], and τ_M is the relaxation time, the time taken for the dipoles to return to its original random orientation. The values of β of the studied films were found and presented in Table 2 with the help of following relation [5].

$$\beta = \frac{1.14}{\text{FWHM}}, \quad (4)$$

where FWHM is the peak full width at half maximum. In addition, τ_M has been found, see Table 2, by using the following Equation [58].

$$\tau_M = 1/\omega_{\max}, \quad (5)$$

where $\omega_{\max}$ is the angular frequency at which the relaxation peak appears. The decrease in τ_M for Cr/blend and Co/blend infers that the complexing with these salts enhances the cooperative segmental motion of the blend chains which may be due to an increase in free volume in the polymer matrix. Finally, the M''- M' plot for the pure blend, the inset, and blend/salt films is depicted in Fig. 12. As obvious, semicircles behavior was observed through the whole frequencies. Complexing $CrNO_3$ and $CoNO_3$ reduce the radius of these semi-circles which confirm an increase in the ionic conductivity [14].

4 Conclusion

Pure PVC/PMMA membranes and that loaded with 10 wt% of Cd, Co, Cr or Mg nitrate salt were prepared and investigated, as a comparative study. The improvements in the optical and dielectric properties of the samples were explained based on the modifications induced in the structure and morphology of the blend after adding the salts. XRD and FTIR spectroscopy showed an increase in the amorphous nature and complexation between the nitrate salts and the blend. SEM analysis showed significant morphological changes in

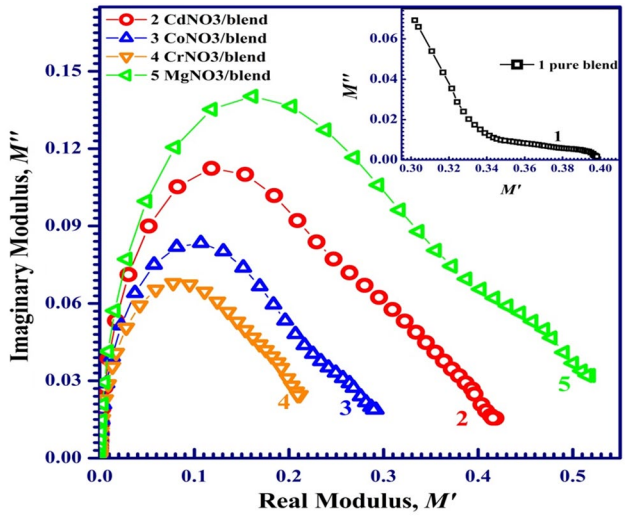

Fig. 12 Frequency dependent-electrical modulus plane plots, the imaginary M'' versus real M' of the pure blend and electrolyte films

the films' surface and porosity. DSC analysis reveals the decrease in T_m values with complexing with different metal nitrate salts. Such decrease confirms the interaction between metal salts with PVC/PMMA blend matrix. The prepared membranes exhibit high transmittance, 50–85% in the visible and near IR regions. $CoNO_3$ and $CrNO_3$ greatly reduced the direct (indirect) E_g of the blend from 4.9 eV (4.3 eV) to 3.7 eV (2.1 eV) and 3.4 eV (1.9 eV), respectively. This means increasing the semiconducting behavior of the composites. The dielectric constant (ε') and dissipation factor (tan δ) of the pure blend were 2.89 and 0.03 and increased with complexing nitrate salts. AC conductivity (σ_{ac}) show two regions, frequency independent plateau region and significant increase of σ_{ac} with f region. σ_{ac} increases with complexing nitrate in the ascending order $MgNO_3$, $CdNO_3$, $CoNO_3$, and $CrNO_3$ salt doped films. Non-Debye type conductivity relaxation was found from the electrical modulus formalism. Finally, a decrease in the relaxation time (τ_M) for Cr/blend and Co/blend compared with other salts was reported. In short sentences, introducing Co, Cr or Mg salts produce porous membranes valid for water filtration application. The significant reduction in E_g of the blend with maintaining a relatively high transmittance encourage the utilization of these membranes for some optoelectronic applications. Moreover, Cr and Co salts exhibited the higher impact on the optical and electric properties of the blend, and this make these composites candidate for Cr and Co battery applications.

Acknowledgements The authors gratefully acknowledge the approval and the support of this research study by the Grant no. 7662-SCI-2018-3-9-F from the Deanship of the Scientific Research at Northern Border University, Arar, K.S.A.

References

1. C.M.S. Prasanna, S.A. Suthanthiraraj, Investigations of zinc ion dissociation in gel polymer electrolytes based on poly(vinyl chloride) and poly(ethyl methacrylate) blend on the addition of two different ceramic nanofillers. J. Inorg. Organomet. Polym Mater. **29**(2), 483–501 (2019)
2. D. Vanitha, S.A. Bahadur, N. Nallamuthu, S. Athimoolam, A. Manikandan, Electrical impedance studies on sodium ion conducting composite blend polymer electrolyte. J. Inorg. Organomet. Polym Mater. **27**(1), 257–265 (2017)
3. N.S. Alghunaim, Spectroscopic analysis of PMMA/PVC blends containing $CoCl_2$. Res. Phys. **5**, 331–336 (2015)
4. C. Du, C. Liu, X. Yin, Effect of cooling mode on anodic bonding properties of solid polymer electrolytes. J. Inorg. Organomet. Polym Mater. **28**(1), 146–151 (2018)
5. K. Gohel, D.K. Kanchan, Ionic conductivity and relaxation studies in PVDF-HFP:PMMA-based gel polymer blend electrolyte with $LiClO_4$ salt. J. Adv. Dielectr. **8**(1), 1850005 (2018)
6. Y.P. Mahant, S.B. Kondawar, D.V. Nandanwar, P. Koinkar, Poly(methyl methacrylate) reinforced poly(vinylidene fluoride) composites electrospun nanofibrous polymer electrolytes as potential separator for lithium ion batteries. Mater. Renew. Sustain. Energy **7**, 5 (2018)
7. K. Omri, R. Lahouli, Tunable dielectric and microstructure properties Zn_2SiO_4–Mn glass–ceramics for multifunctional applications. J. Mater. Sci. **30**, 7834–7839 (2019)
8. K. Omri, R. Lahouli, L. El Mir, Microstructure and electrical properties of silica-Zn_2SiO_4-Mn glass-ceramics as composite for optoelectronic devices. Res. Phys. **12**, 2141–2145 (2019)
9. H. Abomostafa, S.A. Gad, A.I. Khalaf, Improving the optical, mechanical and dielectric properties of PMMA: $Mg_{1-x}Cu_xO$ based polymer nanocomposites. J. Inorg. Organomet. Polym Mater. **28**(6), 2759–2769 (2018)
10. M.I. Mohammed, Optical properties of ZnO nanoparticles dispersed in PMMA/PVDF blend. J. Mol. Struct. **1169**, 9–17 (2018)
11. F. Avelino, D.R. de Oliveira, S.E. Mazzetto, D. Lomonaco, Poly(methyl methacrylate) films reinforced with coconut shell lignin fractions to enhance their UV-blocking, antioxidant and thermomechanical properties. Int. J. Biol. Macromol. **125**, 171–180 (2019)
12. L.-F. Fang, B.-K. Zhu, L.-P. Zhu, H. Matsuyama, S. Zhao, Structures and antifouling properties of polyvinyl chloride/poly(methyl methacrylate)-graft-poly(ethylene glycol) blend membranes formed in different coagulation media. J. Membr. Sci. **524**, 235–244 (2017)
13. S.V. Kuppu, A.R. Jeyaraman, P.K. Guruviah, S. Thambusamy, Preparation and characterizations of PMMA-PVDF based polymer composite electrolyte materials for dye sensitized solar cell. Curr. Appl. Phys. **18**, 619–625 (2018)
14. N.S. Alghunaim, Structural, thermal, dielectric spectroscopic and AC impedance properties of SiC nanoparticles doped PVK/PVC blend. Res. Phys. **9**, 1136–1140 (2018)
15. M. Dinari, N. Roghani, Calcium iron layered double hydroxide/poly(vinyl chloride) nanocomposites: synthesis, characterization and Cd^{2+} removal behavior. J. Inorg. Organomet. Polym. (2019). https://doi.org/10.1007/s10904-019-01265-2
16. B.S. Dizajikan, M. Asadollahi, S.A. Musavi, D. Bastani, Preparation of poly(vinyl chloride) (PVC) ultrafiltration membranes from PVC/additive/solvent and application of UF membranes as substrate for fabrication of reverse osmosis membranes. J. Appl. Polym. Sci. **135**, 46267 (2018)
17. D. Ghazanfari, D. Bastani, S.A. Mousavi, Preparation and characterization of poly(vinyl chloride) (PVC) based membrane for wastewater treatment. J. Water Process Eng. **16**, 98–107 (2017)

18. M. Arsalan, Rafiuddin, synthesis, characterization and electrochemical observation of PVC based ZMP composite porous membrane and its physicochemical studies by applying some strong electrolytes through TMS equation. J. Solid State Electrochem. **19**(8), 2283–2290 (2015)
19. M. Arsalan, M.M.A. Khan, Rafiuddin, A comparative study of theoretical, electrochemical and ionic transport through PVC based $Cu_3(PO_4)_2$ and polystyrene supported $Ni_3(PO_4)_2$ composite ion exchange porous membranes. Desalination **318**, 97–106 (2013)
20. D.M. da Silva Freitas, P.L. Araujo, E.S. Araujo, K.A.D.S. Aquino, Effect of copper sulfide nanoparticles in poly(vinyl chloride) exposed to gamma irradiation. J. Inorg. Organomet. Polym Mater. **27**(5), 1546–1555 (2017)
21. A. Bhran, A. Shoaib, D. Elsadeq, A. El-gendi, H. Abdallah, Preparation of PVC/PVP composite polymer membranes via phase inversion process for water treatment purposes. Chin. J. Chem. Eng. **26**, 715–722 (2018)
22. L. Klapiszewski, J. Tomaszewska, K. Skórczewska, T. Jesionowski, Preparation and characterization of eco-friendly $Mg(OH)_2$/lignin hybrid material and its use as a functional filler for poly(vinyl chloride). Polymers **9**, 258 (2017)
23. M. Arsalan, F. Alam, I. Khan, M. Oves, Synthesis and characterization of $Co_3(Po_4)_2$ and $Ni_3(Po_4)_2$ composite membranes based on PVC: a comparative electrochemical studies through aqueous electrolyte solutions. J. Membr. Sci. Res. **4**, 41–50 (2018)
24. M. Zhao, X. Zuo, X. Ma, X. Xiao, J. Liu, J. Nan, Self-supported PVdF/P(VC-VAc) blended polymer electrolytes for $LiNi_{0.5}Mn_{1.5}O_4$/Li batteries. J. Membr. Sci. **532**, 30–37 (2017)
25. J.D. Honeycutt, A theoretical study of tacticity effects on poly(vinyl chloride)/poly(methyl methacrylate) miscibility. Macromolecules **27**(19), 5377–5381 (1994)
26. D.F. Varnell, E.J. Moskala, P.C. Painter, M.M. Coleman, On the application of fourier transform infrared spectroscopy to the elucidation of specific interactions in miscible polyester-poly(vinyl chloride) blends. Polym. Eng. Sci. **23**, 658–662 (1983)
27. Z. Zhong, Q. Cao, X. Wang, N. Wu, Y. Wang, PVC–PMMA composite electrospun membranes as polymer electrolytes for polymer lithium-ion batteries. Ionics **18**, 47–53 (2012)
28. S. Ramesh, C. Liew, Dielectric and FTIR studies on blending of [xPMMA–(1–x)PVC] with LiTFSI. Measurement **46**, 1650–1656 (2013)
29. S. Ramesh, K.H. Leen, K. Kumutha, A.K. Arof, FTIR studies of PVC/PMMA blend based polymer electrolytes. Spectrochim. Acta A **66**, 1237–1242 (2007)
30. M.S. Khan, R. Gul, M.S. Wahid, Studies on thin films of PVC-PMMA blend polymer electrolytes. J. Polym. Eng. **33**(7), 633–638 (2013)
31. M. Khutia, G.M. Joshi, Dielectric relaxation of PVC/PMMA/NiO blends as a function of DC bias. J. Mater. Sci. **26**(7), 5475–5488 (2015)
32. A.M. El Sayed, W.M. Morsi, Dielectric relaxation and optical properties of polyvinyl chloride/lead monoxide nanocomposites. Polym. Compos. **34**(12), 2031–2039 (2013)
33. S. Khursheed, P. Biswas, V.K. Singh, V. Kumar, H.C. Swart, J. Sharma, Synthesis and optical studies of $KCaVO_4$:Sm^{3+}/PMMA nanocomposites. Vacuum **159**, 414–422 (2019)
34. J. Joseph, K. Deshmukh, K. Chidambaram, M. Faisal, E. Selvarajan, K.K. Sadasivuni, M.B. Ahamed, S.K.K. Pasha, Dielectric and electromagnetic interference shielding properties of germanium dioxide nanoparticle reinforced poly(vinyl chloride) and poly(methylmethacrylate) blend nanocomposites. J. Mater. Sci. **29**(23), 20172–20188 (2018)
35. R. Arunkumar, R.S. Babu, M.U. Rani, Investigation on Al_2O_3 doped PVC–PBMA blend polymer electrolytes. J. Mater. Sci. **28**, 3309–3316 (2017)
36. T. Mzir, M.W. Khemici, M. Dahmane, M. Mzir, N. Doulache, Dielectric characterization of polyvinyl chloride/polymethyl methacrylate (PVC/PMMA) blends by TSDC technique. Int. J. Polym. Anal. Charact. **23**(8), 675–683 (2018)
37. S.S. Suresh, S. Mohanty, S.K. Nayak, Preparation and characterization of recycled blends using poly(vinyl chloride) and poly(methyl methacrylate) recovered from waste electrical and electronic equipments. J. Clean. Prod. **149**, 863–873 (2017)
38. M. Yanilmaz, X. Zhang, Polymethylmethacrylate/polyacrylonitrile membranes via centrifugal spinning as separator in li-ion batteries. Polymers **7**, 629–643 (2015)
39. S. El-Gamal, A.M. El Sayed, E.E. Abdel-Hady, Effect of cobalt oxide nanoparticles on the nano-scale free volume and optical properties of biodegradable CMC/PVA films. J. Polym. Environ. **26**(6), 2536–2545 (2018)
40. C. Subbu, S. Rajendran, K. Kesavan, C.M. Mathew, Lithium ion conduction in PVdC-co-AN based polymer blend electrolytes doped with different lithium salts. Int. Polym. Process. **4**, 476–486 (2015)
41. T. Liu, J. Petermann, Multiple melting behavior in isothermally cold-crystallized isotactic polystyrene. Polymer **42**, 6453–6461 (2001)
42. K. Yamani, R. Berenguer, A. Benyoucef, E. Morallon, Preparation of polypyrrole (PPy)-derived polymer/ZrO_2 nanocomposites. J. Therm. Anal. Calorim. **135**, 2089–2100 (2019)
43. V.S. Sangawar, N.A. Moharil, Study of electrical, thermal and optical behavior of polypyrrole filled PVC:PMMA thin film thermoelectrets. Chem. Sci. Trans. **1**(2), 447–455 (2012)
44. R. Nadimicherla, R. Kalla, R. Muchakayala, X. Guo, Effects of potassium iodide (KI) on crystallinity, thermal stability, and electrical properties of polymer blend electrolytes (PVC/PEO:KI). Solid State Ionics **278**, 260–267 (2015)
45. A.M. El Sayed, M. Shaban, Morphological, surface and optical properties of spin-coated IrOx films; influence of spin speed, annealing and (Cr, La) codoping. Ceram. Int. **45**(7), 8460–8470 (2019)
46. S. El-Gamal, A.M. El Sayed, Physical properties of the organic polymeric blend (PVA/PAM) modified with MgO nanofillers. J. Compos. Mater. **53**(20), 2831 (2019)
47. A.M. El Sayed, S. El-Gamal, Synthesis and investigation of the electrical and dielectric properties of Co_3O_4/(CMC + PVA) nanocomposite films. J. Polym. Res. **22**(5), 97 (2015)
48. M.S. El-Bana, A.M. El Gh Mohammed, S.El-Gamal Sayed, Preparation and characterization of PbO/carboxymethyl cellulose/polyvinylpyrrolidone nanocomposite films. Polym. Compos. **39**(10), 3712–3725 (2018)
49. Y. Seki, R. Kita, N. Shinyashiki, S. Yagihara, M. Yoneyama, Molecular dynamics of poly(methyl methacrylate) determined by dielectric relaxation spectroscopy. AIP Conf. Proc. **1518**, 466–469 (2013)
50. N. Kulshrestha, B. Chatterjee, P.N. Gupta, Characterization and electrical properties of polyvinyl alcohol based polymer electrolyte films doped with ammonium thiocyanate. Mater. Sci. Eng., B **184**, 49–57 (2014)
51. S.B. Aziz, Z.H.Z. Abidin, Electrical conduction mechanism in solid polymer electrolytes: new concepts to arrhenius equation. J. Soft Matter (2013). https://doi.org/10.1155/2013/323868
52. A.K. Jonscher, *Universal Relaxation Law* (Chelsea Dielectrics Press, London, 1992)
53. L.N. Sim, S.R. Majid, A.K. Arof, FTIR studies of PEMA/PVdF-HFP blend polymer electrolyte system incorporated with $LiCF_3SO_3$ salt. Vib. Spectrosc. **58**, 57–66 (2012)
54. A. Bello, E. Laredo, M. Grimau, Comparison of analysis of dielectric spectra of PCL in the ε^* and the M^* formalism. J. Non Cryst. Solids **353**, 4283–4287 (2007)

55. S. El-Gamal, A.M. Ismail, R. El-Mallawany, Dielectric and nanoscale free volume properties of polyaniline/polyvinyl alcohol nanocomposites. J. Mater. Sci.: Mater. Electron. **26**(10), 7544–7553 (2015)
56. R.J. Sengwa, S. Sankhla, Ionic conduction and dielectric dispersion study on chain dynamics of poly(vinyl pyrrolidone)-glycerol blends. Ind. J. Pure Appl. Phys. **46**(7), 513–520 (2008)
57. A. Karmakar, A. Ghosh, Dielectric permittivity and electric modulus of polyethylene oxide (PEO)-$LiClO_4$ composite electrolytes. Curr. Appl. Phys. **12**, 539–543 (2012)
58. Y.T. Ravikiran, M.T. Lagare, M. Sairam, N.N. Mallikarjuna, B. Sreedhar, S. Manohar, A.G. MacDiarmid, T.M. Aminabhavi, Synthesis, characterization and low frequency AC conduction of polyaniline/niobium pentoxide composites. Synth. Met. **156**(16–17), 1139–1147 (2006)